Journal of Sustainable Metallurgy
https://doi.org/10.1007/s40831-026-01463-6

RESEARCH ARTICLE

Utilization Potential of Steel Slag for CO_2 Sequestration and as a Filler Aggregate in Mortars

Mojca Loncnar[1] · Sara Tominc[2] · Lea Žibret[2] · Sabina Dolenec[2,3] · Maruša Mrak[2] · Vilma Ducman[2]

Received: 29 August 2025 / Accepted: 13 February 2026

Abstract

Steel slag is an abundant by-product of steelmaking and a promising candidate for CO_2 sequestration due to its favorable chemical composition and mineralogy. In this study, the CO_2 sequestration capacity of the processed steel slag Ekominit was analyzed. Ekominit is a mineral product obtained by processing a mixture of electric arc furnace (EAF) stainless steel slag and ladle slag, currently used only for simple engineering constructions. The study demonstrated a promising sequestration capacity of 127.4 g CO_2 per kg of Ekominit, measured using direct semi-dry carbonation under ambient pressure at 40 ± 0.5 °C, 80 ± 3.2% relative humidity, and 20 ± 0.1 vol% CO_2 for 5 days, which is within the typical range reported for carbonated steel slags (100–150 g_{CO2}/ kg_{slag}). Although Ekominit did not show sufficient potential as a supplementary cementitious material in mortar, the results confirmed that its incorporation as a filler—with or without carbonation treatment—enhances both the flowability and compressive strength of the mortar. This research emphasizes the dual-function potential of Ekominit: it captures CO_2, contributing to the decarbonization of the steel sector, and enables its reuse in construction materials, even improving the performance of mortars when using such carbonated Ekominit as fillers. Through such industrial symbiosis, environmental impact is further reduced by substituting virgin raw materials with secondary products.

Graphical Abstract

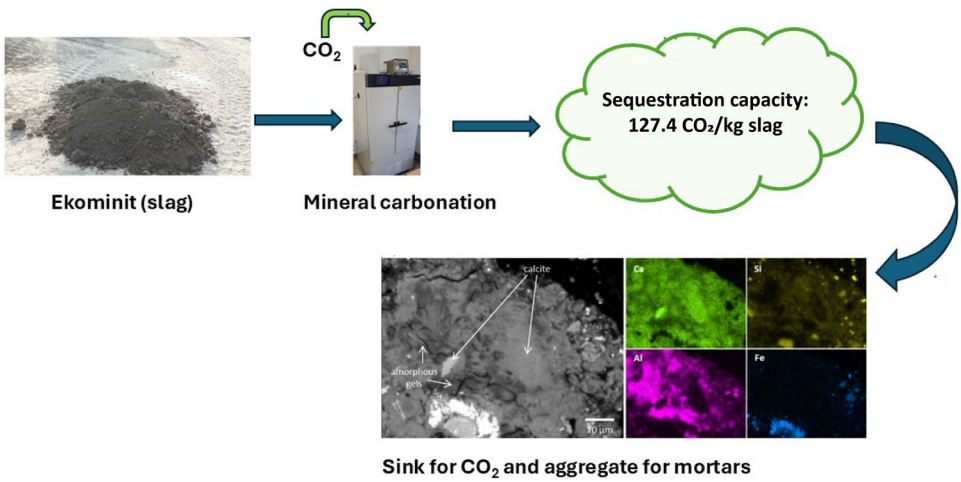

Keywords Electric arc furnace (EAF) steel slag · Ladle slag · Mineral carbonation · CO_2 sequestration · Carbonated materials · Filler aggregate · Mortar performance · Sustainable construction materials

The contributing editor for this article was U. Pal.

Extended author information available on the last page of the article

Published online: 27 February 2026

Introduction

Recently, carbon mineralization has emerged as an alternative strategy to CO_2 injection and long-term subsurface storage, known as geologic carbon storage (GCS); both approaches mitigate climate destabilization caused by high-energy-related CO_2 emissions [1–3]. Carbon mineralization, also called CO_2 mineral carbonation, is a straightforward approach for CO_2 capture and storage. It is one of several approaches to CO_2 sequestration, involving the reaction of CO_2 with alkaline materials rich in Ca- and Mg (hydr)oxides and silicates, which lead to the formation of stable, solid carbonate products [1, 4–6]. Although only a limited number of pilot sites for carbon mineralization are currently operating, the technology shows potential as a cost-effective CO_2 sequestration method compared to alternative approaches. At the CarbFix pilot project in Iceland [2, 7], at least 95% of the injected CO_2 was mineralized to carbonate minerals within two years, with estimated costs of $20–30 per ton of CO_2. In contrast, Blondes et al. [8] reported that in situ CO_2 mineralization in basaltic rocks could cost between $30 and $100 per ton of CO_2. Ex situ carbonation of CaO- and MgO-rich industrial wastes, ultramafic mine tailings, or steel slag offers lower cost estimates, around $8 per ton of CO_2 captured [8], highlighting the economic potential of mineralization in industrial residues compared to in situ approaches. A comprehensive assessment of global CO_2 mitigation via mineralization and utilization of alkaline solid wastes indicates that approximately 310 Mt CO_2 of reductions can be achieved through direct mineralization. Iron and steel slags represent the major source (43.5%), followed by cement-derived wastes (16.3%), mining wastes (13.5%), and coal combustion ash (12.3%) [9].

Steel slag, a by-product of steel production, is considered a promising material for CO_2 mineralization due to its wide availability, composition, and mineralogy, which enable the production of value-added products while permanently storing CO_2 [10, 11]. Studies have shown that carbonation of steelmaking slags can reduce almost 12–17% of CO_2 emissions from the iron and steel industry [12]. Steel slags are rich in Ca, Si, Fe, and Mg and contain minerals that favor carbonation, including silicates, aluminosilicates, free CaO, and free MgO [13]. The primary residues from steelmaking are basic oxygen furnace (BOF) and electric arc furnace (EAF) slags, while secondary steelmaking mainly generates ladle and argon oxygen decarburisation (AOD) slags. Steel slag typically consists of 85–90% mineral components, with the remainder comprising metallic components. Variations in steelmaking processes lead to differences in slag chemistry and mineralogy, as summarized in Table 1 [14].

The steel slag can undergo CO_2 mineralization through either direct or indirect carbonation. Indirect carbonation is a two-step process involving metal leaching from the slag, followed by CO_2 dissolution to form carbonates. Direct carbonation, in contrast, is a single step, with CO_2 reacting directly with the slag without leaching, making it a more economical approach [6, 12, 13, 15, 16]. The primary minerals in steel slag that react with CO_2 are CaO, f-MgO, $Ca(OH)_2$, $Mg(OH)_2$, and silicate phases such as C_2S and C_3S, as summarized in Eqs. (1–6) [13, 16].

Table 1 Typical steelmaking slag composition range (wt%), adopted from Ref. [14]

Component	BOF slag	EAF slag	Secondary steelmaking slag	AOD slag
CaO	45–54	25–35	30–52	48–68
SiO_2	11–18	8–18	8–23	20–40
Al_2O_3	1–5	3–10	3–20	1–2.5
MgO	1–6	2–9	6–12	4–6
Total Fe	14–22	20–30	0.5–12	0.4–2
Total Mn	1–5	2–8	0.5–3	0.6–1.0 (MnO)
Total Cr	0.1–0.3	0.5–2.2	< 0.1–0.5	0.1–5 (Cr_2O_3)

$$CaO\,(s) + CO_2(g) \rightarrow CaCO_3 \tag{1}$$

$$MgO\,(s) + CO_2(g) \rightarrow CaCO_3 \tag{2}$$

$$Ca(OH)_2(s) + CO_2(g) \rightarrow CaCO_3(s) + H_2O\,(l) \tag{3}$$

$$Mg(OH)_2(s) + CO_2(g) \rightarrow MgCO_3(s) + H_2O\,(l) \tag{4}$$

$$\frac{1}{3}\left(3CaO \cdot SiO_2\right)(s) + CO_2(g) \rightarrow CaCO_3(s) + \frac{1}{3}SiO_2(s) \tag{5}$$

$$\frac{1}{2}\left(2CaO \cdot SiO_2\right)(s) + CO_2(g) \rightarrow CaCO_3(s) + \frac{1}{2}SiO_2(s) \tag{6}$$

The carbonation process is similar to natural weathering, occurring rapidly for Ca-containing oxides, while Mg oxides react more slowly [17]. Steel slags can also contain a significant proportion of the RO phase [16]. Carbonation has been shown to enhance hydration of this phase by promoting Mg leaching through CO_2 dissolution [18]. However, the exact reaction mechanisms remain insufficiently understood.

Several studies have shown that one ton of steel slag can sequester up to 250 kg of CO_2 [9, 19, 20]. In an experiment by Biava et al. [21], a NaOH solution was first acidified by CO_2 injection before slag addition, which accelerated the carbonation reaction. Slags sourced from various European steel production facilities demonstrated CO_2 capture of 100–240 g CO_2 per kg of slag, with uptake strongly

influenced by slag chemistry and mineralogy. Bonenfant et al. [20] reported that ladle slag exhibited a CO_2 uptake of 247 g CO_2 per kg of slag, which was 14 times higher than that of the EAF slag, in aqueous suspension using 99.5% purity CO_2. Under varying carbonation conditions, continuous casting (CC) slag was found to carbonate more extensively than AOD stainless steel slag under nearly all processing conditions, due to differences in particle microstructure. Optimal pressurized slurry carbonation achieved CO_2 uptakes of 310 g/kg for CC slag and 260 g/kg for AOD slag [13]. Similarly, Linz–Donawitz slag carbonated in autoclave reactors under controlled L/S ratios, temperature, and CO_2 pressure showed comparable sequestration capacities [22].

Direct dry carbonation of steel slag offers rapid CO_2 sequestration, low raw material costs, and strong potential for waste heat utilization, making it a promising approach for in situ carbon capture in the steel industry. Under typical flue gas conditions at 600 °C, the process can achieve a maximum CO_2 sequestration capacity of 88.5 g CO_2 per kg of slag [23]. The semi-dry carbonation process offers additional advantages: solid particles can absorb a thin layer of moisture, allowing CO_2 gas to dissolve and react within this surface layer. This enables high degrees of carbonation over shorter reaction times, improving overall cost-effectiveness [24]. Librandi et al. [11] reported that BOF slags exhibit higher reactivity toward CO_2 compared with EAF slags. The CO_2 uptake of moisturized BOF and EAF slags was evaluated under a 100% CO_2 atmosphere at 50 °C and pressures of 1.3 or 10 bar. After 4 h, the moisturized BOF slag showed CO_2 uptakes ranging from 18 to 22% (at 1.3 and 10 bar, respectively), while the moisturized EAF slag showed uptakes of 11.2% to 11.9% under the same conditions. As flue gases generally contain lower CO_2 concentrations and CO_2 capture is expensive and not yet widely integrated into existing processes, diluted CO_2 streams currently have greater potential for industrial application. Quaghebeur et al. [25] demonstrated that BOF slag and stainless steel (SS) slag with 10 wt% moisture, carbonated at moderate pressure (2.0 MPa) with CO_2 feed gas concentrations of 20%–77% and temperatures between 20 and 140 °C, were able to sequester 100–150 g of CO_2 per kg of slag.

In concrete and mortar, steel slag can be reused as a cement component after appropriate grinding [26]. Steel slag contains mineralogical phases similar to those in Portland cement clinker, such as C_3S ($3CaO{\cdot}SiO_2$), C_2S ($2Ca{\cdot}SiO_2$), and C_2F ($2CaO{\cdot}Fe_2O_3$), making it a potential supplementary cementitious material (SCM). However, its reactivity is limited: C_3S is present in low proportions, the hydration of C_2S and the amorphous phase becomes significant only after approximately 7 days, and the high iron content in C_2F reduces its reactivity [21]. If carbonation can be used to convert steel slag into a cementitious material, it has the potential to significantly reduce emissions associated with the concrete industry [8]. During carbonation, the alkaline components within slag particles dissolve, leading to the formation of a calcium-depleted amorphous aluminosilicate gel on the particle surface. When not obstructed by a newly formed calcite layer, this gel can participate in cement hydration, enhancing the effectiveness of steel slag as an SCM [27].

Ground steel slag can be used as a filler in concrete or mortar mixes to balance particle size distribution when aggregates lack sufficient fines. Fine aggregates primarily fill the voids within coarse aggregates and improve the workability of the concrete mix [28]. Moosberg-Bustnes [28] reported that mortar containing fines (45 µm fraction) from disintegrated AOD slag exhibited slightly higher compressive strength than reference samples containing quartz, likely due to a filler effect or a positive chemical interaction. However, the use of steel slag as a filler may be limited by the presence of free calcium oxide (f-CaO) and/or free magnesium oxide (f-MgO) [29]. During later stages of hydration, these compounds form calcium hydroxide ($Ca(OH)_2$) and magnesium hydroxide ($Mg(OH)_2$), resulting in significant volume expansions of 98% and 148%, respectively [30, 31]. Bertos et al. [32] showed that carbonation can enhance both the physical and chemical properties of steel slag aggregate while fixing CO_2 within the slag, providing a new pathway for its utilization. Wang et al. [33] investigated mixtures of gypsum, steel slag, and water, showing that gypsum improves both the compressive strength of steel slag and its CO_2 absorption, as confirmed by microscopic analysis. Although recent studies [34–36] have demonstrated that carbonation technology can improve the strength and stability of concrete containing treated steel slag, the effects of carbonation on finely granulated steel slag used as a filler in cement or mortar mixtures have been poorly investigated and require further study.

This study aims to assess the performance of processed steel slag Ekominit in mortar, either as an SCM or as a filler. The carbon-negative product was produced via mineral carbonation under mild conditions, at ambient temperature and atmospheric pressure. For the carbonated slag with most particles smaller than 125 µm, the SCM potential was evaluated, while mortar mixtures containing carbonated aggregates were assessed for their properties in both fresh and hardened states. This paper presents a novel dual-function approach for Ekominit use: first, as a CO_2 capture material, and second, as a sustainable input for the construction sector, specifically as a filler in mortar.

Experimental

Raw Materials

The Ekominit sample, produced from processed EAF-S and ladle slag, was provided by SIJ Acroni, Slovenia. Ekominit is processed in the slag processing line into a fine-grained wet material similar to wet sand [37]. It is used for simple engineering constructions and all types of construction embankments, except in frozen zones.

Characterization of Ekominit

Before chemical analysis, the samples were dried at 105 °C and ground to a particle size below 125 µm. The loss on ignition (LOI) of the raw materials was determined at 950 °C in accordance with the EN 196–2:2013 standard [38]. The chemical composition was determined by X-ray fluorescence (XRF) using an ARL PERFORM'X spectrometer (Thermo Fisher Scientific Inc., Ecublens, Switzerland) operated with UniQuant 5 software (Thermo Fisher Scientific Inc., Waltham, MA, USA). Measurements were performed on fused beads, prepared by melting a mixture of ignited samples with Fluxana (Li-tetraborate and Li-metaborate mixed in a 1:1 mass ratio) at a ratio of 1:10. An aqueous LiBr solution (7.5 g LiBr (s) from Sigma Aldrich dissolved in 50 mL H_2O) was added to the mixture.

Prior to X-ray powder diffraction (XRD) analysis, the samples were ground to below 63 µm in an agate mortar and backloaded into a circular sample holder. XRD was performed on a PANalytical X'Pert Pro X-ray powder diffractometer using CuKα1 radiation and an X'Celerator detector at 45 kV and 40 mA. The scan range was 5–75°, with a step size of 0.017° 2θ, a 1° divergence slit, and a 15 mm mask. Rietveld refinement was used to quantify phases with PANalytical X'Pert High Score Plus diffraction software (version 4.9).

Particle size distributions of the as-received and carbonated Ekominit samples, as well as the CEN standard fraction (< 125 µm), were determined using a laser particle analyzer (Malvern Mastersizer X). Prior to measurements, the powders were ultrasonically dispersed in isopropanol. The specific surface area of the as-received and carbonated Ekominit samples and the CEN standard fraction (< 125 µm) was measured by nitrogen adsorption measurements at 77 K using the Brunauer–Emmett–Teller (BET) method with a Micromeritics ASAP-2020 analyzer. The specific density of the materials was determined using a gas pycnometer (Ultrapyc 1200e).

For microstructural characterization, the < 125 µm fraction of the as-received and carbonated Ekominit samples was mixed with epoxy resin and dry-polished to obtain cross-sections for scanning electron microscopy (SEM). Both the polished cross-sections and unpolished powder samples (adhered to carbon tape) were coated with a carbon layer (~ 35 nm thick). SEM observations and energy dispersive X-ray spectroscopy (EDXS) analyses were performed using a JEOL IT500 LV SEM equipped with an Ultim Max detector (Oxford Instruments) at 15 kV in high-vacuum mode, and data were processed with Aztec 5.0 SP1 software (Oxford Instruments Nanotechnology Tools Ltd).

Sequestration Potential of Ekominit

Direct semi-dry carbonation of Ekominit was performed using a modified method proposed by Tominc and Ducman [39]. The samples were sieved to < 125 µm, and about 20 g of each was placed in a closed carbonation chamber at ambient pressure under controlled conditions (40 ± 0.5 °C, relative humidity (RH) 80 ± 3.2%, and 20 ± 0.1 vol% CO_2). Carbonation progress was monitored by weighing the samples before and after 1, 2, 3, and 5 days of curing, until complete carbonation was achieved. At each weighing, the $CaCO_3$ content was determined using a calcimeter. After complete carbonation, the samples were dried at 105 °C for 24 h before further analysis.

The CO_2 content (wt%) of the as-received and carbonated Ekominit samples was determined by thermogravimetric analysis (TGA) and calcimetry. Carbonate content was measured using a pressure calcimeter (OFITE Recording Calcimeter with DAQ, OFI Testing Equipment, Inc., Houston, TX, USA) in accordance with ASTM D 4373. A 1.0 ± 0.001 g sample was reacted with 20 ± 0.01 mL of 10% HCl in a closed reaction, and the evolved CO_2 pressure was recorded. All samples were dried and sieved to < 125 microns prior to measurement. The CO_2 content in Ekominit was calculated from the measured pressure using the stoichiometric ratios given in Eq. (7).

$$CaCO_3 + 2HCl \rightarrow CaCl_2 + CO_2 + H_2O \quad (7)$$

TGA was performed on dried samples using a TGA Q5000IR thermal analyzer (TA Instruments, New Castle, Delaware, USA) over the temperature range 25–1000 °C at a heating rate of 10 K min^{-1}. To avoid oxidation, the sample chamber was purged with nitrogen at 25 mL min^{-1}. Sample masses of 10–20 mg were placed in 100 µL Al_2O_3 crucibles. The CO_2 content (wt%) was calculated from the mass loss within the temperature interval corresponding to carbonate decomposition, relative to the dry mass at 105 °C. Data were processed using TA Universal Analysis 2000 software v.4.5A (TA Instruments, New Castle, Delaware, USA).

CO_2 uptake was calculated by calcimetric measurements and TGA based on Eq. (8), reported in several recent studies [11, 40, 41]:

$$CO_2 \text{ uptake (wt\%)} = \left(\frac{CO_{2,\ \text{carbonated slag(wt\%)}} - CO_{2,\ \text{as-received slag (wt\%)}}}{100 - CO_{2,\ \text{carbonated slag (wt\%)}}} \right) \times 100 \quad (8)$$

The CO_2 sequestration capacity of Ekominit was calculated based on Eq. (9) [31]:

$$CO_2 \text{capacity} \left(\frac{g_{CO_2}}{kg_{slag}} \right) = \left(\frac{CO_{2,\ \text{carbonated slag (wt\%)}}}{100 - CO_{2,\ \text{carbonated slag (wt\%)}}} \right) \times 1000 \quad (9)$$

Preparation of Mortar Mixtures

To investigate the influence of Ekominit as an SCM and/or filler, samples of the as-received and carbonated Ekominit were ground to below 125 µm.

Test Methods for Properties in the Fresh State and Hardened State

The reactivity of the as-received and carbonated Ekominit was determined by isothermal calorimetry according to the standard test method ASTM C1897-20 [42] using a Thermometric TAM Air (TA Instruments). This method assesses the chemical (pozzolanic or hydraulic) reactivity of SCMs by measuring heat release over 7 days.

The soundness was evaluated in accordance with EN 196–3 [43] by preparing a mixture of 30% as-received or carbonated Ekominit and 70% CEM I 42.5N cement. In accordance with the standard, the soundness must not exceed 10 mm during the test.

The strength activity index (SAI) of the Ekominit samples was determined in accordance with EN 450–1 [44]. Mortar mixtures were prepared with 25% of the cement replaced by either as-received or carbonated Ekominit and tested in accordance with EN 196–1 [45]. The SAI, defined as the ratio of the compressive strength of a mortar containing 25% Ekominit as SCM to that of a control mortar, must be at least 75% at 28 days and 85% at 90 days.

Furthermore, mortar mixtures were produced with Ekominit added in the same quantity as the CEN standard sand fraction of < 125 µm, and the total aggregate quantity was reduced accordingly to achieve a cement-to-aggregate ratio of 1:3. It was found that this proportion of CEN standard sand was 4%. The water-to-cement ratio of the mortar was 0.5, and CEM I 42.5N was used. For the reference sample, standard mortar was prepared using CEM I 42.5N. The samples were mixed as specified in the EN 197–1 standard [46]. The flow behavior of the mortar with incorporated Ekominit was determined according to EN 1015–3 [47] on two samples.

To determine compressive and flexural strength, the mortar mixture was poured into prismatic molds measuring 4 × 4 × 16 cm. After 24 h, the mortar samples were demolded and cured in a humid chamber at 20 ± 1 °C and 95% relative humidity until testing under laboratory conditions. Compressive and flexural strength measurements were performed after 28 days on three prisms using a ToniNORM testing device (ToniTechnic from Zwick) at a loading rate of 0.05 kN s^{-1}.

Results and Discussion

Characterization of Ekominit

The characterization of Ekominit was evaluated prior to carbonation, with its CaO content being particularly important as it determines the extent of carbonation [48]. XRF analysis of the as-received Ekominit shows that it is mainly composed of CaO (36.9 wt%), SiO_2 (18.3 wt%), Al_2O_3 (10.2 wt%), MgO (14 wt%), and Fe_2O_3 (7.2 wt%), with lower contents of Cr_2O_3 (2.8 wt%) and MnO (1.6 wt%). The main oxide contents, determined by XRF and loss on ignition (LOI) at 950 °C, are listed in Table 1. Compared with Carbinox stainless steel slag, Ekominit has lower SiO_2 content but higher Fe_2O_3 and Al_2O_3 contents,

Table 2 Characterization of Ekominit, including its chemical composition (determined by XRF analysis in wt%), LOI (wt%), specific surface area (BET), and specific density, with the reported chemical composition of Carbinox provided for comparison (n.d. indicates not determined) [49]

Sample	LOI $_{950\,°C}$	CaO	SiO_2	MgO	Al_2O_3	Fe_2O_3	FeO	Cr_2O_3	MnO	BET (m^2/g)	Specific density (g/cm^3)	D_{50} (µm)	D_{90} (µm)
Ekominit	7.5	36.9	18.3	14.0	10.2	7.2	-	2.8	1.6	10.63	3.02	25.4	101.6
Carbinox	n.d	40.0	37.0	13.0	5.5	0.0	0.54	2.1	0.77	n.d	n.d	n.d	n.d

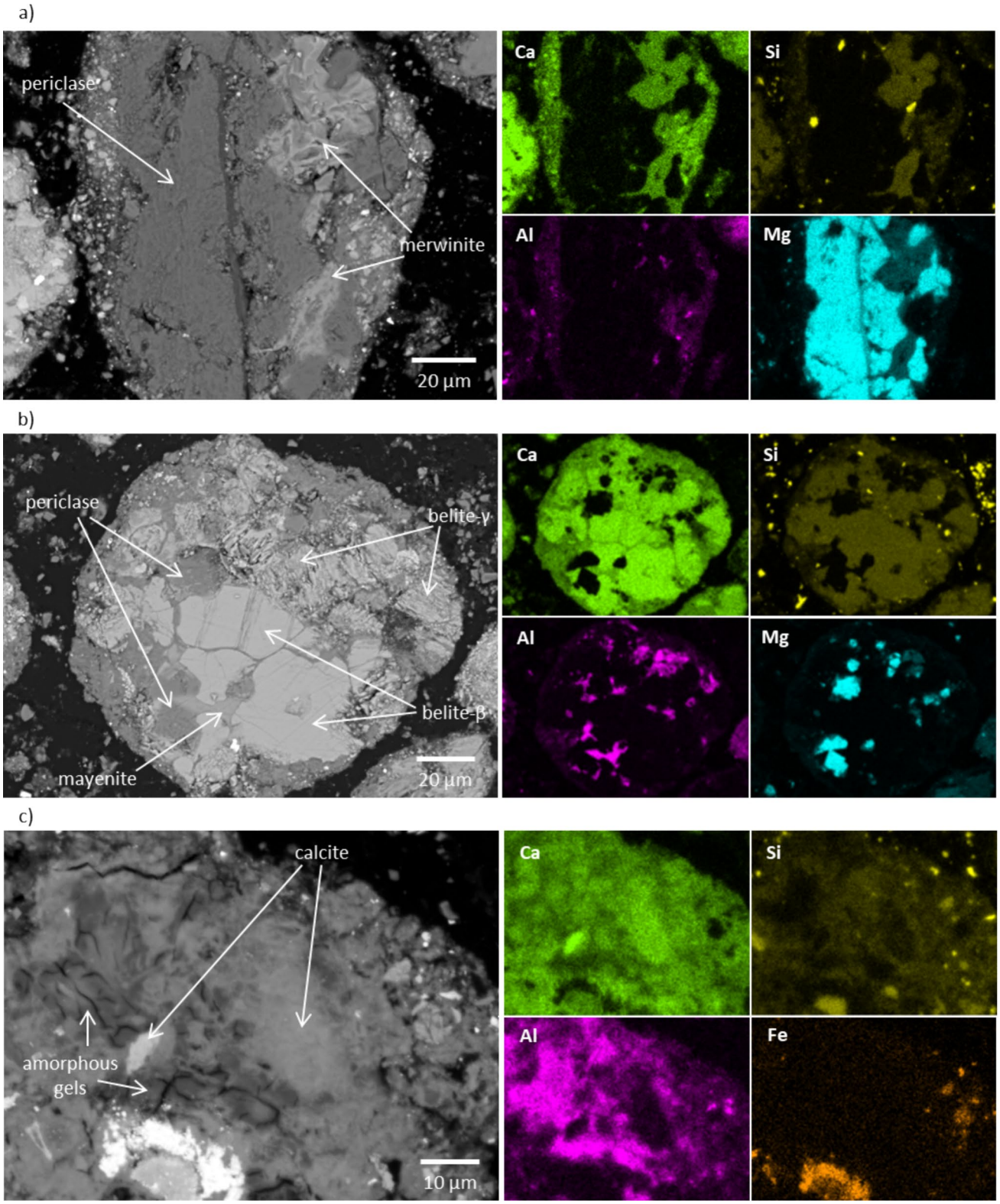

Fig. 1 Elemental EDXS maps for the as-received (**a**) and carbonated (**b**, **c**) Ekominit, showing the main phases

while CaO and MgO contents are similar, as shown in Table 2 [49]. (Fig. 1).

As Ekominit forms during the wet processing of the mixture of EAF-S slag and ladle slag, it is highly exposed to water, so hydration of a hydraulic phase, such as belite, can already occur during slag processing. Some of these hydration products are non-crystalline (e.g., C-S-H, AFm phases), which appear as an amorphous phase in X-ray diffraction (XRD) analysis but are visible by TG. The TG/DTG and SEM/EDXS analyses of Ekominit (Fig. 2 and 3) confirm the presence of hydration products.

SEM/EDXS and XRD results (Fig. 1 and 3) showed that Ekominit consisted mainly of belite (including γ-C_2S and β-C_2S), merwinite, and periclase. Other phases present in larger amounts include calcite, ferrite, mayenite, and enstatite. Minor phases (below 2 wt%) present in the sample are Friedel's salt, spinel, brucite, and quartz. As a result of slag processing, the Ekominit hydrates and forms a range of secondary phases such as katoite, calcium silicate hydrate (C–S–H), calcium–aluminum–silicate–hydrate (C–A–S–H), and AFm phases.

Sequestration Potential of Ekominit

Thermogravimetric analysis measures the mass change of a sample under controlled atmosphere, with results shown in Table 2. The mass loss from room temperature to 105 °C is attributed to free water and the initial dehydration of amorphous or poorly crystalline calcium silicate hydrates (C-S-H) [41, 50]. The results also indicate that the as-received Ekominit contains AFm phases (such as monosulfate, monocarbonate, or Friedel's salt), identifiable as a mass loss in the region between 140 and 400 °C [51]. Mass loss from 420 to 800 °C corresponds to the decomposition of $CaCO_3$ into CaO and CO_2 and provides information on the amount of sequestered CO_2 in Ekominit (Fig. 2).

The CO_2 uptake was determined by calcimetric and TGA calculations (Table 2), with results differing by 2% [52]. This

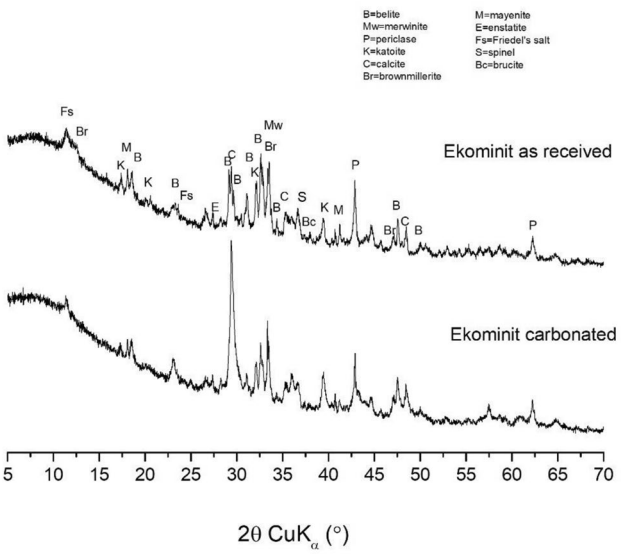

Fig. 3 X-ray diffraction patterns of the as-received and carbonated Ekominit

difference may be due to the amount of sample used (1 g for calcimetric measurements and 10–20 mg for TGA) or from overlapping decomposition peaks in TGA, which can make the carbonate decomposition range difficult to define accurately [53]. In such cases, calcimetric measurements may be more reliable; however, the measurement uncertainty of the pressure calcimeter may be 2% [54]. Based on the calcimetric calculations, the CO_2 uptake for Ekominit was 8.7 wt% (Table 2), indicating that Ekominit can sequester 127.4 g_{CO2}/kg_{slag}, which falls within the range of values reported in the literature (100–150 g_{CO2}/kg_{slag}) [25].

A comparison of the as-received and carbonated Ekominit indicates the influence of carbonation on the mineralogical composition. As shown in Fig. 3, carbonation-susceptible phases decrease as carbonation progresses, indicating their conversion into carbonation products. The results show a reduction mainly in the amounts of belite, periclase, merwinite, brucite, and katoite due to carbonation.

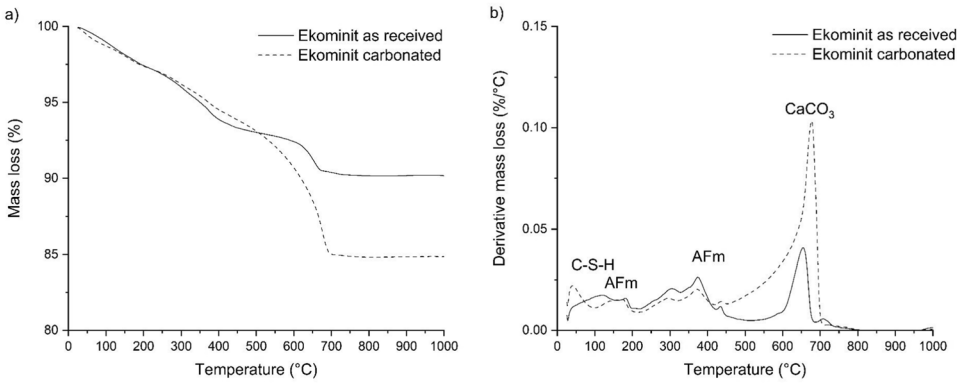

Fig. 2 **a** TG and **b** DTG curves of the as-received and carbonated Ekominit

Furthermore, the formation of calcite becomes more pronounced, reflecting its role as the principal carbonation product.

Ca- and Mg-bearing oxides (such as brucite and periclase in Ekominit) and hydroxides have shown greater effectiveness in sequestering CO_2 than many other mineral phases [55]. These compounds readily react with CO_2 to form calcite ($CaCO_3$) [12]. Ca-containing phases such as belite can also react with CO_2 to form carbonates [12]. In the presence of water and CO_2, γ-C_2S, along with any unreacted β-C_2S, can undergo carbonation reactions, producing both C–S–H and $CaCO_3$ [13]. As shown in Table 3, the γ-C_2S in the carbonated Ekominit increased. Chang et al. [46] found that CO_2 uptake by γ-C_2S is more pronounced than by β-C_2S, resulting in 18. 5% CO_2 uptake and the formation of carbonated products such as calcite and Si-gel phase [56]. Other Ca-rich phases, such as merwinite, exhibit relatively low reactivity under carbonation conditions [57] but can also dissolve in the presence of CO_2, especially under elevated humidity and prolonged reaction times, contributing to carbonate and aluminosilicate gel formation.

The amount of ACn, represented mostly by C–S–H and C–A–S–H in the carbonated Ekominit sample, does not change significantly, as C–S–H continues to undergo carbonation. This process involves the decalcification of C–S–H, ultimately leading to the formation of silica gel (SiO_2) and calcium carbonate [58].

Additives in Mortars

Assessment of SCM Potential

Firstly, both the as-received and carbonated Ekominit have been assessed for their potential as SCMs; therefore, the SAI test and calorimetry were carried out. The SAI test confirms SCM potential by comparing a sample containing 25 wt% Ekominit with a sample containing only CEM1 (reference material). The activity index should be at least 75% after 28 days and 85% after 90 days. As shown in Fig. 4, both the as-received and carbonated Ekominit exhibited activity index values below these limits.

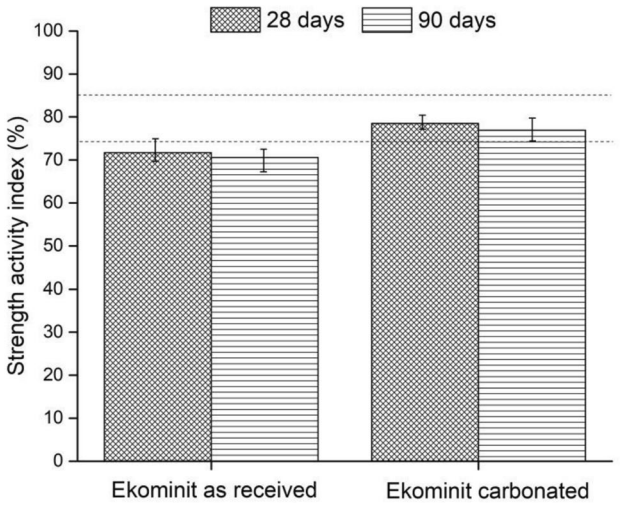

Fig. 4 Strength activity index (SAI) at 28 and 90 days of the as-received and carbonated Ekominit

In addition, Table 4 and Fig. 5 show the heat flow and cumulative heat release of Ekominit before and after carbonation over 7 days. The initial peak, observed immediately after mixing, corresponds to material wetting and dissolution. A main peak, indicating the reaction between the sample and $Ca(OH)_2$, occurred after 25 h for the as-received Ekominit and earlier, after 8 h, for carbonated Ekominit. The cumulative heat was almost the same for the as-received and carbonated Ekominit, with only slightly higher values observed for carbonated Ekominit, indicating there is almost no difference in reactivity between non-carbonated and carbonated Ekominit. The experimental results indicate that Ekominit exhibits limited potential compared to other SCMs. The cumulative heat release of the as-received and carbonated Ekominit measured after 3 and 7 days of hydration is significantly lower than that of other SCMs such as calcined clays, fly ash, and pozzolans [59], suggesting that the material has limited reactivity. In comparison to the slag tested in the Li et al. [59] study, where the results of the R3 reactivity tests showed cumulative heat after 3 and 7 days in the range of 432.4 J/g to 454.1 J/g and 503.8 J/g to 558.8 J/g, respectively, the results obtained for Ekominit

Table 3 CO_2 content (wt%) in the as-received and carbonated Ekominit, determined by TGA and calcimeter and calculated CO_2 uptake and CO_2 sequestration capacity

Sample		TGA		TGA calculations			Calcimetric calculations			
		H_2O (wt%)	CO_2 (wt%)	dry matter (wt%)	CO_2/dry matter (wt%)	CO_2 uptake (wt%)	$CaCO_3$ (wt%)	CO_2 (wt%)	CO_2 uptake (wt%)	CO_2 seq. capacity (g_{CO2}/kg_{slag})
Ekominit	as-received	1.9	3.5	98.1	3.6	-	8.2	3.6	-	-
	carbonated	1.9	9.4	98.1	9.6	**6.7**	25.6	11.3	**8.7**	**127.4**

Table 4 Phase composition of the as-received and carbonated Ekominit

Mineral	Formula	Ekominit as-received (wt%)	Ekominit carbonated (wt%)
Belite-beta	β-Ca_2SiO_4	4.5	5.2
Belite-gamma	γ-Ca_2SiO_4	8.2	5.3
Merwinite	$Ca_3Mg(SiO_4)_2$	6.2	2.1
Periclase	MgO	4.5	3.2
Ferrite	$Ca_2(Al,Fe)_2O_5$	2.9	2.3
Mayenite	$12CaO{\cdot}7Al_2O_3$	2.6	3.0
Enstatite	$MgSiO_3$	2.4	4.3
Spinel	$MgAlFeO_4$	1.1	0.7
Katoite	$Ca_3Al_2(OH)_{12}$	3.7	1.0
Friedel's salt	$Ca_2Al(OH)_6(Cl,OH) \cdot 2 H_2O$	1.7	0.6
Brucite	$Mg(OH)_2$	1.0	0.5
Calcite	$CaCO_3$	3.3	13.1
Nesquehonite	$MgCO_3 \cdot 3H_2O$	0.0	0.1
ACn*		57.6	58.3
Gof		2.3	2.2
Rwp		5.3	4.9

*ACn: Amorphous and crystalline non-quantifiable phases

(Table 5) were much lower. This value also falls below the typical ranges reported for other SCMs, which are approximately 50–300 J/g for pozzolans, 160–360 J/g for fly ashes, 250–960 J/g for calcined clays, and 350–630 J/g for silica fumes [60]. Therefore, it is likely that Ekominit does not meet the criteria to be considered as an effective SCM.

Application of Ekominit as Filler Aggregate in Mortars

Both the as-received and carbonated Ekominit were used as filler aggregate in mortar mixtures. The reference mixture was prepared with CEN aggregate, while a cement-to-aggregate ratio of 1:3 was obtained in a mixture of Ekominit. The proportion of added Ekominit sample was equal to the fine CEN standard sand fraction (< 125 µm), i.e., 4 wt%.

Figure 6 shows the particle size distribution of the as-received and carbonated Ekominit compared with the reference CEN. As expected, the particle size distribution of the as-received and carbonated Ekominit does not differ, whereas the CEN has a coarser particle size distribution, which is also confirmed by BET (Table 6). BET measurements of carbonated Ekominit show a significant increase in surface area compared to Ekominit in its original state. According to the literature, this is due to the chemical reaction of CO_2 with the slag, which creates new pore structures and expands existing ones [61] (Fig. 7). In addition, carbonation can partially break down the C–S–H gel network, the phase present in the studied processed slag, releasing silica-rich gels or leaving behind high-surface-area amorphous silica [62].

To assess the effect of carbonation on the stability of the sample, the volume expansion of the cement paste with standard consistency was observed using the relative movement of two needles. The requirement according to standard EN 196–3 [43] is less than 10 mm. Despite the presence of potentially harmful phases in the slag, such as f-MgO [63], the soundness of both the as-received and carbonated samples remains very low (Table 7), indicating that the amount present is insufficient to cause any negative impact.

The results of the flow measurements are given in Table 8. The addition of Ekominit as fine aggregate, both as-received and carbonated, increases the workability of

Table 5 Cumulative heat (J/g) after 3 and 7 days of hydration, normalized to the weight of the as-received Ekominit and carbonated Ekominit

	3 days (J/g)	7 days (J/g)
Ekominit as-received	66.03	81.81
Ekominit carbonated	66.34	82.46

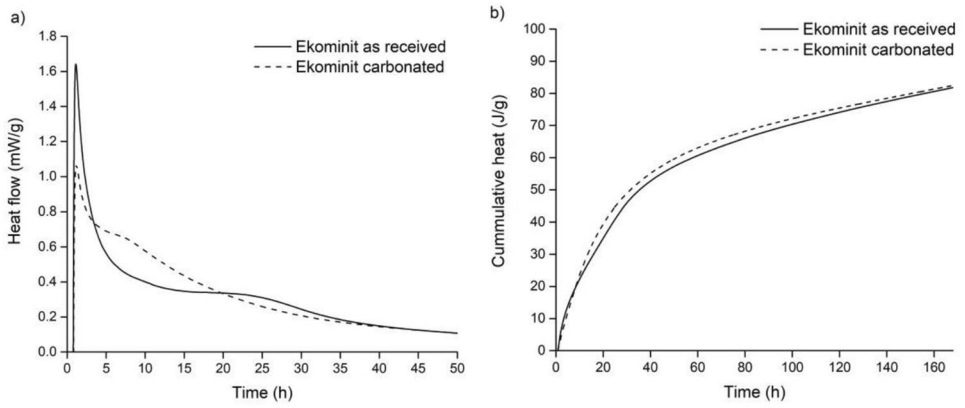

Fig. 5 Heat flow (**a**) and cumulative heat development (**b**) for the as-received and carbonated Ekominit, with both values normalized to the sample weight

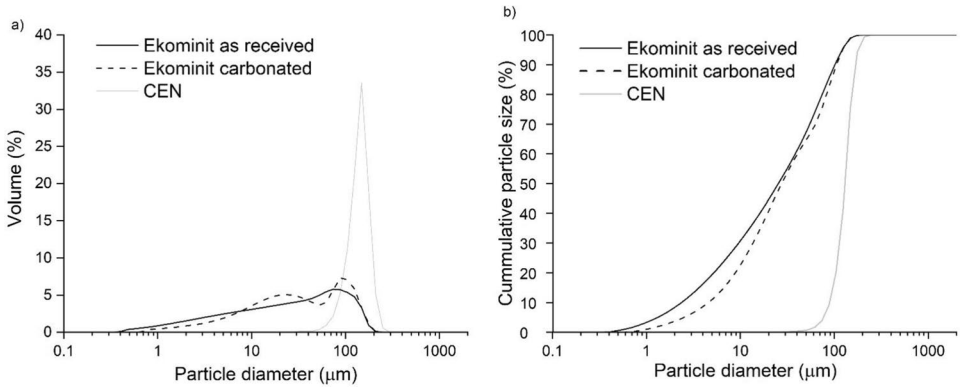

Fig. 6 Particle size distribution of the as-received and carbonated Ekominit and CEN standard: **a** volume and **b** cumulative particle size

Table 6 BET surface area and specific density of the as-received and carbonated Ekominit (ground below 125 µm) and CEN standard (sieved below 125 µm)

	BET (m^2/g)	Specific density (g/cm^3)
Ekominit fresh (< 125 µm)	10.63	3.02
Ekominit carbonated (< 125 µm)	24.44	2.86
CEN (< 125 µm)	0.28	2.67

mortars compared to the reference, which is attributed to reduced internal friction, allowing the mortar to flow more easily. Along with its grading, the cohesiveness and tendency to act as ball bearings for larger particles make fine aggregates a better indicator of workability [64]. Moderate amounts of fines generally improve workability, while increasing amounts of fines raise the amount of water required to adequately wet the particle surfaces and maintain a specified workability [65]. Despite the higher specific BET surface area of carbonated Ekominit, its workability is not reduced compared to Ekominit as-received. Using carbonated Ekominit as a filler represents added value, as it also acts as a CO_2 sink.

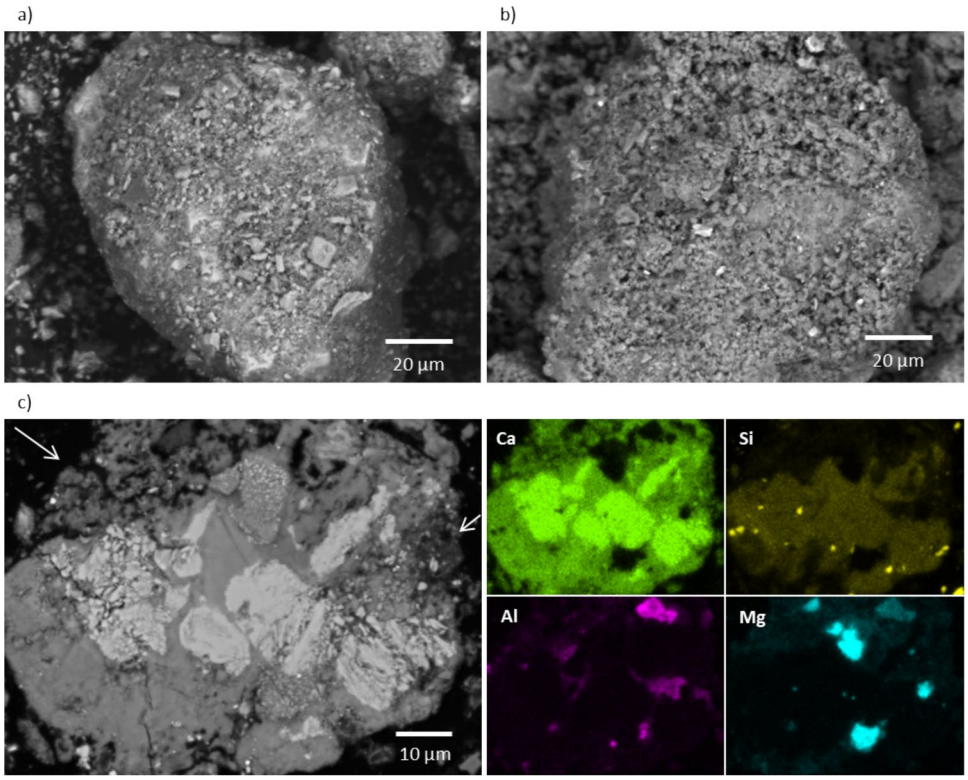

Fig. 7 Comparison of the surface of unpolished as-received (**a**) and carbonated (**b**) Ekominit by SEM, and the porous outer layer (see white arrows) of carbonated Ekominit in polished cross-section—elemental EDXS maps (**c**)

Table 7 Soundness of a mixture of 30% as-received or carbonated Ekominit and 70% CEM I 42.5N cement

	Soundness (mm)
Ekominit as-received	0.3
Ekominit carbonated	0.6

Table 8 Flow values of the mortar mixture of Ekominit as-received, Ekominit carbonated, and the reference (standard mortar)

	Flow (mm)
Ekominit as-received	177 ± 1.0
Ekominit carbonated	177 ± 1.5
Reference	173 ± 1.0

Table 9 Compressive and flexural strength after 28 days for mortar mixtures with Ekominit as-received, carbonated Ekominit, and the reference (standard mortar)

	Compressive strength [N/mm^2]	Flexural strength [N/mm^2]
Ekominit as-received	47.8 ± 0.8	7.2 ± 0.3
Ekominit carbonated	49.3 ± 1.5	7.2 ± 0.3
Reference	45.6 ± 1.7	7.6 ± 0.1

The results showed that the addition of both the as-received and carbonated Ekominit led to higher compressive strength than the reference sample (Table 9). Carbonated Ekominit exhibited a slightly higher compressive strength than Ekominit in its as-received state, which can be attributed to its finer particle size distribution. This finer distribution enhances compressive strength due to the particle packing effect [66, 67]. Even with the addition of only 4 wt% carbonated Ekominit to the mixture, compressive strength increased by more than 8% compared to the reference sample. In both cases, flexural strength was slightly lower than that of the reference sample (Table 9), indicating a slight decrease in toughness.

Conclusions

Ekominit, a mineral product obtained by processing a mixture of stainless EAF slag and ladle slag, was characterized and investigated for its sequestration capacity and potential use in the construction sector. Ekominit contains the following carbonatable minerals: belite, periclase, merwinite, brucite, and katoite. It was confirmed that Ekominit is capable of binding up to 127.4 g CO_2 per kg of Ekominit, which is comparable to the amounts reported in the literature for carbonatable materials. Ekominit has also been evaluated as an additive in mortars, where it was found that it cannot serve as a reactive SCM, but it can still replace some of the natural aggregate (filler aggregate) without compromising performance. In fact, when CEN sand in mortars is partially replaced by Ekominit (with or without carbonation pretreatment), the influence of this additive on selected properties in the fresh state, such as workability, or on the mechanical properties in the hardened state, is even slightly positive. With such an integrated approach, we contribute to the decarbonization of the steel sector through carbon sequestration and also promote circular economy principles by valorizing secondary materials to replace virgin raw resources, thereby substantially reducing the overall environmental footprint of the industry.

Further investigations will be carried out through a systematic study to determine how much virgin aggregate can be replaced by Ekominit, and how this replacement affects the durability of such mixtures.

Funding This research was funded by EIT RawMaterials, grant number 21107 (Georis), and by the Slovenian Research and Innovation Agency (ARIS) under research core grant no. P2-0273.

References

1. Alturki A (2022) The global carbon footprint and how new carbon mineralization technologies can be used to reduce CO_2 emissions. ChemEngineering 6(3):44. https://doi.org/10.3390/chemengineering6030044
2. Matter JM, Stute M, Snaebjornsdottir SO, Oelkers EH, Gislason SR, Aradottir ES, Sigfusson B, Gunnarsson I, Sigurdardottir H, Gunnlaugsson E, Axelsson G, Alfredsson HA, Wolff-Boenisch D, Mesfin K, Taya DF, Hall J, Dideriksen K, Broecker WS (2016) Rapid carbon mineralization for permanent disposal of anthropogenic carbon dioxide emissions. Science 352:1312–1314. https://doi.org/10.1126/science.aad8132
3. McGrail BP, Schaef HT, Spane FA, Horner JA, Owen AT, Cliff JB, Qafoku O, Thompson CJ, Sullivan EC (2017) Wallula basalt

pilot demonstration project: post-injection results and conclusions. Energy Procedia 114:5783–5790. https://doi.org/10.1016/j.egypro.2017.03.1716
4. Koch R, Sailer G, Paczkowski S, Pelz S, Poetsch J, Müller J (2021) Lab-scale carbonation of wood ash for CO_2-sequestration. Energies 14(21):7371. https://doi.org/10.3390/en14217371
5. Li L, Wu M (2022) An overview of utilizing CO_2 for accelerated carbonation treatment in the concrete industry. J CO2 Util 60:102000. https://doi.org/10.1016/j.jcou.2022.102000
6. Saran RK, Arora V, Yadav S (2018) CO_2 sequestration by mineral carbonation: a review. Glob NEST J 20(3):497–503. https://doi.org/10.30955/gnj.002597
7. Matter JM, Broecker WS, Gislason SR, Gunnlaugsson E, Oelkers EH, Stute M, Sigurdardóttir H, Stefansson A, Alfreðsson HA, Aradóttir ES, Axelsson G, Sigfússon B, Wolff-Boenisch D (2011) The carbFix pilot project-storing carbon dioxide in basalt. Energy Procedia 4:5579–5585. https://doi.org/10.1016/j.egypro.2011.02.546
8. Blondes MS, Merrill MD, Anderson ST, DeVera CA (2019) Carbon dioxide mineralization feasibility in the United States: US geological survey. Sci Investig Rep 2018-5079. https://doi.org/10.3133/sir20185079
9. Pan S-Y, Chen Y-H, Fan L-S, Kim H, Gao X, Ling T-C, Chiang P-C, Pei S-L, Gu G (2020) CO_2 mineralization and utilization by alkaline solid wastes for potential carbon reduction. Nat Sustain 3:399–405. https://doi.org/10.1038/s41893-020-0486-9
10. Santos RM, Van Bouwel J, Vandevelde E, Mertens G, Elsen J, Van Gerven T (2013) Accelerated mineral carbonation of stainless steel slags for CO_2 storage and waste valorization: effect of process parameters on geochemical properties. Int J Greenhouse Gas Control 17:32–45. https://doi.org/10.1016/j.ijggc.2013.04.004
11. Librandi P, Nielsen P, Costa G, Snellings R, Quaghebeur M, Baciocchi R (2019) Mechanical and environmental properties of carbonated steel slag compacts as a function of mineralogy and CO_2 uptake. J CO2 Util 33:201–214. https://doi.org/10.1016/j.jcou.2019.05.028
12. Chen Z, Cang Z, Yang F, Zhang J, Zhang L (2021) Carbonation of steelmaking slag presents an opportunity for carbon neutral: a review. J CO2 Util 54:101738. https://doi.org/10.1016/j.jcou.2021.101738
13. Wang S, Wang M, Liu F, Song Q, Deng Y, Ye W, Ni J, Si X, Wang C (2024) A review on the carbonation of steel slag: properties, mechanism, and application. Materials 17(9):2066. https://doi.org/10.3390/ma17092066
14. Brand AS, Fanijo EO (2020) A review of the influence of steel furnace slag type on the properties of cementitious composites. Appl Sci 10(22):8210. https://doi.org/10.3390/app10228210
15. Ashraf W, Olek J (2018) Carbonation activated binders from pure calcium silicates: reaction kinetics and performance controlling factors. Cem Concr Compos 93:85–98. https://doi.org/10.1016/j.cemconcomp.2018.07.004
16. DiGiovanni C, Hisseine OA, Awolayo AN (2024) Carbon dioxide sequestration through steel slag carbonation: review of mechanisms, process parameters, and cleaner upcycling pathways. J CO2 Util 81:102736. https://doi.org/10.1016/j.jcou.2024.102736
17. Lackner KS, Wendt CH, Butt DP, Joyce EL, Sharp DH (1995) Carbon dioxide disposal in carbonate minerals. Energy 20(11):1153–1170. https://doi.org/10.1016/0360-5442(95)00071-N
18. Li W, Cao M, Wang D, Chang J (2023) Increase in volume stability of RO phases in steel slag by combined treatment of alkali and dry carbonation. Constr Build Mater 396:132345. https://doi.org/10.1016/j.conbuildmat.2023.132345
19. Wang X, Lu X, Turvey CC, Dipple GM, Ni W (2022) Evaluation of the carbon sequestration potential of steel slag in China based on theoretical and experimental labile Ca. Resour Conserv Recycl 186:106590. https://doi.org/10.1016/j.resconrec.2022.106590
20. Bonenfant D, Kharoune L, Sauve´ S, Hausler R, Niquette P, Mimeault M, Kharoune M (2008) CO_2 sequestration potential of steel slags at ambient pressure and temperature. Ind Eng Chem Res 47:7610–7616. https://doi.org/10.1021/ie701721j
21. Biava G, Zajac M, Principallo A, Depero LE, Haha MB, Bontempi E (2025) Evaluation of steel slags in CO_2 sequestration and as supplementary cementitious material. Constr Build Mater 489:142271. https://doi.org/10.1016/j.conbuildmat.2025.142271
22. Huijgen WJJ, Comans RNJ (2006) Carbonation of steel slag for CO_2 sequestration: leaching of products and reaction mechanisms. Environ Sci Technol 40:2790–2796. https://doi.org/10.1021/es052534b
23. Tian S, Jiang J, Chen X, Yan F, Li K (2013) Direct gas-solid carbonation kinetics of steel slag and the contribution to insitu sequestration of flue gas CO_2 in steel-making plants. Chemsuschem 6:2348–2355. https://doi.org/10.1002/cssc.201300436
24. Zajac M, Skibsted J, Bullerjahn F, Skocek J (2022) Semi-dry carbonation of recycled concrete paste. J CO2 Util 63:102111. https://doi.org/10.1016/j.jcou.2022.102111
25. Quaghebeur M, Nielsen P, Horckmans L, Van Mechelen D (2015) Accelerated carbonation of steel slag compacts: development of high-strength construction materials. Front Energy Res 3:52. https://doi.org/10.3389/fenrg.2015.00052
26. Rashad AM (2025) Behavior of steel slag aggregate in mortar and concrete - a comprehensive overview. J Build Eng 53:104536. https://doi.org/10.1016/j.jobe.2022.104536
27. Srivastava S, Cerutti M, Nguyen H, Carvelli V, Kinnunen P, Illikainen M (2023) Carbonated steel slags as supplementary cementitious materials: reaction kinetics and phase evolution. Cem Concr Compos 142:105213. https://doi.org/10.1016/j.cemconcomp.2023.105213
28. Moosberg-Bustnes H. (2004). Steel-slag as filler material in concrete. VII International Conference on Molten Slags Fluxes and Salts, The South African Institute of Mining and Metallurgy.
29. Ren Z, Li D (2023) Application of steel slag as an aggregate in concrete production: a review. Materials 16(17):5841. https://doi.org/10.3390/ma16175841
30. Li M, Lu Y, Yang S, Chu J, Liu Y (2023) Study on the early effect of excitation method on the alkaline steel slag. Sustainability 15(6):4714. https://doi.org/10.3390/su15064714
31. Andrade HD, de Carvalho JMF, Costa LCB, da Fonseca Elói FP, do Carmo e Silva KD, Peixoto RAF (2021) Mechanical performance and resistance to carbonation of steel slag reinforced concrete. Constr Build Mater 298:123910. https://doi.org/10.1016/j.conbuildmat.2021.123910
32. Fernández Bertos M, Simons SJR, Hills CD, Carey PJ (2004) A review of accelerated carbonation technology in the treatment of cement-based materials and sequestration of CO_2. J Hazard Mater 112:193–205. https://doi.org/10.1016/j.jhazmat.2004.04.019
33. Wang X, Ni W, Li J, Zhang S, Hitch M, Pascual R (2019) Carbonation of steel slag and gypsum for building materials and associated reaction mechanisms. Cem Concr Res 125:105893. https://doi.org/10.1016/j.cemconres.2019.105893
34. Liu P, Zhang M, Mo L, Zhong J, Xu M, Deng M (2022) Probe into carbonation mechanism of steel slag via FIB-TEM: the roles of various mineral phases. Cem Concr Res 162:106991. https://doi.org/10.1016/j.cemconres.2022.106991
35. Mo L, Zhang F, Deng M, Jin F, Al-Tabbaa A, Wang A (2017) Accelerated carbonation and performance of concrete made with steel slag as binding materials and aggregates. Cem Concr Compos 83:138–145. https://doi.org/10.1016/j.cemconcomp.2017.07.018
36. Liu P, Zhong J, Zhang M, Mo L, Deng M (2021) Effect of CO_2 treatment on the microstructure and properties of steel

slag supplementary cementitous materials. Constr Build Mater 309:125171. https://doi.org/10.1016/j.conbuildmat.2021.125171
37. Fidanchevski E, Šter K, Mrak M, Rajacic M, Koszo BD, Ipavec A, Teran K, Žibret G, Jovanov V, Aluloska NS, Loncar M, Žibret L, Dolenec S (2024) Characterization of Al-containing industrial residues in the ESEE region supporting circular economy and the EU green deal. Materials 17(24):6245. https://doi.org/10.3390/ma17246245
38. EN 196–2 (2013) Method of testing cement—Part 2: chemical analysis of cement
39. Tominc S, Ducman V (2023) Methodology for evaluating the CO_2 sequestration capacity of waste ashes. Materials 16(15):5284. https://doi.org/10.3390/ma16155284
40. Nielsen P, Quaghebeur M (2023) Determination of the CO_2 uptake of construction products manufactured by mineral carbonation. Minerals 13(8):1079. https://doi.org/10.3390/min13081079
41. Ferrara G, Belli A, Keulen A, Tulliani JM, Palmero P (2023) Testing procedures for CO_2 uptake assessment of accelerated carbonation products: experimental application on basic oxygen furnace steel slag samples. Construct Build Mater 406:133384. https://doi.org/10.1016/j.conbuildmat.2023.133384
42. ASTM C1897–20 (2020) Standard test methods for measuring the reactivity of supplementary cementitious materials by isothermal calorimetry and bound water measurements
43. EN-196–3 (2017) Methods of testing cement - Part 3: determination of setting times and soundness
44. EN 450–1 (2012) Fly ash for concrete - Part 1: Definition, specifications and conformity criteria
45. EN 196–1, Methods of testing cement - Part 1: Determination of strength (2016).
46. EN 197–1 (2011) Cement – Part 1: composition, specifications and conformity criteria for common cements
47. EN 1015–3 (1999) Methods of test for mortar for masonry-Part3: determination of consistence of fresh mortar (by flow table)
48. Capelo-Avilés S, de Oliveira RT, Gallo Stampino II, Gispert-Guirado F, Casals-Terré A, Giancola S, Galán-Mascarós JR (2024) A thorough assessment of mineral carbonation of steel slag and refractory waste. J CO2 Util 82:102770. https://doi.org/10.1016/j.jcou.2024.102770
49. Kamyab HK, Nielsen P, Van Mierloo P, Horckmans L (2021) Carbstone pavers: a sustainable solution for the urban environment. Appl Sci 11(14):6418. https://doi.org/10.3390/app11146418
50. Liu G, Schollbach K, van der Laan S, Tang P, Florea MVA, Brouwers HJH (2020) Recycling and utilization of high volume converter steel slag into CO_2 activated mortars–the role of slag particle size. Resour Conserv Recycl 160:104883. https://doi.org/10.1016/j.resconrec.2020.104883
51. Scrivener K, Snelling R, Lothenbach B (eds) (2018) A practical guide to microstructural analysis of cementitious materials. CRC Press, Boca Raton
52. Loncnar M, Tominc S, Žibret L, Dolenec S, Mrak M, Ducman V (2025) Evaluation of the potential use of carbonated steel slag as a filler aggregate in mortars. 9th International Slag Valorisation Symposium, Leuven, Belgium 131–135
53. Protić M, Miltojević A, Zoraja B, Raos M, Krstić I (2021) Application of thermogravimetry for determination of carbon content in biomass ash as an indicator of the efficiency of the combustion process. Teh Vjesn 28(5):1762–1768. https://doi.org/10.17559/TV-20200508110940
54. Kavčič N, Tominc S, Žibret L, Žibret G, Kolar M, Ducman V (2025) Comparing methods for determining the CO_2 content in CO_2-sequestering materials and natural rock. Ceramics Int 51(25):43786–43795. https://doi.org/10.1016/j.ceramint.2025.07.109
55. Bobicki ER, Liu Q, Xu Z, Zeng H (2012) Carbon capture and storage using alkaline industrial wastes. Prog Energy Combust Sci 38(2):302–320. https://doi.org/10.1016/j.pecs.2011.11.002
56. Chang J, Fang Y, Shang X (2016) The role of β-C_2S and γ-C_2S in carbon capture and strength development. Mater Struct 49:4417–4424. https://doi.org/10.1617/s11527-016-0797-5
57. Chai YE, Miller QRS, Schaef HT, Barpaga D, Bakhshoodeh R, Bodor M, van Gerven T, Santos RM (2021) Pressurized in situ X-ray diffraction insights into super/ subcritical carbonation reaction pathways of steelmaking slags and constituent silicate minerals. The J Supercrit Fluids 171:105191. https://doi.org/10.1016/j.supflu.2021.105191
58. Morandeau A, Thiéry M, Dangla P (2014) Investigation of the carbonation mechanism of CH and C-S-H in terms of kinetics, microstructure changes and moisture properties. Cem Concr Res 56:153–170. https://doi.org/10.1016/j.cemconres.2013.11.015
59. Li X, Snellings R, Antoni M et al (2018) Reactivity tests for supplementary cementitious materials: RILEM TC 267-TRM phase 1. Mater Struct 51:151. https://doi.org/10.1617/s11527-018-1269-x
60. Londono-Zuluaga D, Gholizadeh-Vayghan A, Winnefeld F et al (2022) Report of RILEM TC 267-TRM phase 3: validation of the R3 reactivity test across a wide range of materials. Mater Struct 55:142. https://doi.org/10.1617/s11527-022-01947-3
61. Elyasi Gomari K, Rezaei Gomari S, Hughes D, Ahmed T (2024) Exploring the potential of steel slag waste for carbon sequestration through mineral carbonation: a comparative study of blast-furnace slag and ladle slag. J Environ Manage 351:119835. https://doi.org/10.1016/j.jenvman.2023.119835
62. Thomas JJ, Chen JJ, Allen AJ, Jennings HM (2004) Effects of decalcification on the microstructure and surface area of cement and tricalcium silicate pastes. Cem Concr Res 34(12):2297–2307. https://doi.org/10.1016/j.cemconres.2004.04.007
63. Borhan TM, Al-Rawi RS (2016) Combined effect of MgO and SO_3 contents in cement on compressive strength of concrete. J Eng Sci 9(4):516–525
64. Murdock LJ (1960) The workability of concrete. Mag Concr Res 12:135–144. https://doi.org/10.1680/macr.1960.12.36.135
65. Celik T, Marar K (1996) Effects of crushed stone dust on some properties of concrete. Cem Concr Res 26(7):1121–1130. https://doi.org/10.1016/0008-8846(96)00078-6
66. Kaliyavaradhan SK, Ling T-C (2017) Potential of CO_2 sequestration through construction and demolition (C & D) waste-an overview. J CO_2 Util 20:234–242. https://doi.org/10.1016/j.jcou.2017.05.014
67. Pushpanathan N, Devamani S, RR Tharini ME (2016) Experimental study of particle packing analysis in steel slag aggregate concrete. Int J Eng Res Technol (IJERT) 4(25):1–4

Authors and Affiliations

Mojca Loncnar[1] · Sara Tominc[2] · Lea Žibret[2] · Sabina Dolenec[2,3] · Maruša Mrak[2] · Vilma Ducman[2]

✉ Vilma Ducman
vilma.ducman@zag.si

[1] SIJ Acroni, Cesta Borisa Kidriča 44, 4270 Jesenice, Slovenia

[2] Slovenian National Building and Civil Engineering Institute, Dimičeva ulica 12, 1000 Ljubljana, Slovenia

[3] Faculty of Natural Sciences and Engineering, University of Ljubljana, Aškerčeva cesta 12, 1000 Ljubljana, Slovenia